

## Functionalized Raspberry-Like Microparticles obtained by Assembly of Nanoparticles during Electrospaying

Eun Chul Cho, Yoon Kyun Hwang,<sup>†</sup> and Unyong Jeong<sup>‡,\*</sup>

*Department of Chemical Engineering, Division of Chemical and Bioengineering, Hanyang University, Seoul 133-791, Korea*  
<sup>†</sup>*Amorepacific Corporation/R&D Center, Yongin 446-729, Korea*

<sup>‡</sup>*Department of Materials Science and Engineering, Yonsei University, Seoul 120-749, Korea. \*E-mail: ujeong@yonsei.ac.kr*  
*Received February 6, 2014, Accepted February 24, 2014*

The present study suggests a novel method to produce raspberry-like microparticles containing diverse functional materials inside. The raspberry-like microparticles were produced from a random assembly of uniformly-sized poly(methyl methacrylate) (PMMA) nanoparticles via electrospaying. The solution containing the PMMA nanoparticles were supplied through the inner nozzle and compressed air was emitted through the outer nozzle. The air supply helped fast evaporation of acetone, so it enabled copious amount of microparticles as dry powder. The microparticles were highly porous both on the surface and interiors, hence various materials with a function of UV-blocking (TiO<sub>2</sub> nanoparticles and methoxyphenyl triazine) or anti-aging (ethyl(4-(2,3-dihydro-1H-indene-5-carboxyamido) benzoate)) were loaded in large amount (17 wt % versus PMMA). The surface and interior structures of the microparticles were dependent on the characteristics of functional materials. The results clearly suggest that the process to prepare the raspberry-like microparticles can be an excellent approach to generate functional microstructures.

**Key Words :** Electrospaying, microparticles, Nanoparticle assembly, Particle functionalization, Polymer particles

### Introduction

Assembled structures of particles often possess not only the characteristics of the nanoparticle but also properties superior to those of bulk materials with equivalent geometries.<sup>1,2</sup> For example, the assembled particles exhibit unique optical properties that individual particles and bulk materials do not have, which are typically observed in colloidal crystals.<sup>3-6</sup> Among the various types of assembled structures, raspberry-like microparticles have attracted much interest because the microparticles mimic self-cleaning function of the natural system.<sup>7,8</sup> Numerous types of raspberry-like structures have been produced through assembly of sub-micron particles on the surfaces of template particles.<sup>9-26</sup> However, the application of the raspberry-like structures has been mostly limited to formation of superhydrophobic surfaces.<sup>22-26</sup> The limited application is mainly attributed to difficulty of functionalization. Unlike the hollow shell microparticles, the raspberry-like particles have been considered that they cannot provide sufficient empty space to encapsulate functional materials such as drug molecules and nanoparticles. Development of a simple method that allow effective loading of functional materials in the raspberry-like particles is expected to expand applications which includes drug delivery systems, catalysis, and optics.<sup>27,28</sup>

In this study, we modified electrospaying to produce raspberry-like structures made of polymer nanoparticles. This process allowed loading a large amount of functional materials that were mixed evenly in the body of the raspberry-like microparticles. When the compatibility of the materials

with the polymer nanoparticles is not good, the functional materials were coated on the surface of the raspberry-like microparticles. This study demonstrates enhanced stability of bioactive drugs stored in the raspberry-like microparticles and exhibits high loading of TiO<sub>2</sub> nanoparticles for UV protection.

### Experimental

**Materials.** Methyl methacrylate (MMA, 99%), ethylene glycol dimethacrylate (EGDMA, 98%), potassium persulfate (KPS, 99%), methylated- $\beta$ -cyclodextrin (M- $\beta$ -CD), and titanium (IV) dioxide (TiO<sub>2</sub>) powder (99%) were purchased from Aldrich and used without purification. Acetone (HPLC grade) was purchased from Fisher Scientific. Methoxyphenyl triazine (Tinosorb<sup>R</sup>-S) was received from BASF. Ethyl(4-(2,3-dihydro-1H-indene-5-carboxyamido) benzoate) was received from Amorepacific Corporation, Korea.

**Synthesis of PMMA Nanoparticles.** Poly(methyl methacrylate) (PMMA) nanoparticles were synthesized according to the literature.<sup>29</sup> Briefly, 100 mL of an M- $\beta$ -CD aqueous solution (1 wt %) was heated to 70 °C, and KPS was added. While stirring, a mixture of 10 mL MMA and EGDMA ([MMA]:[EGDMA] = 9:1) was slowly dropped in the aqueous solution over 1–2 h, and the reaction was then allowed to further proceed for 2 h. The aqueous nanoparticle dispersions were centrifuged and the supernatant was decanted. The centrifuged nanoparticles were re-dispersed in deionized water and centrifuged. This purification procedure was repeated three times. The washed PMMA nanoparticles were

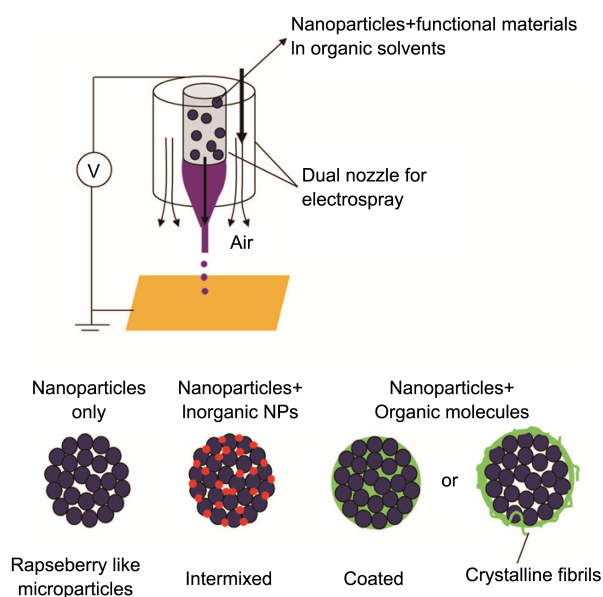


**Figure 1.** A schematic depicting the experimental setup for the production of raspberry-like microparticles containing various functional materials. While maintaining the similar skeletal structures, the surface and interior microstructures of the microparticles were modified depending on the functional materials being incorporated with the polymer nanoparticles (NPs).

dispersed in acetone for electrospaying.

**Preparation of the Raspberry-like PMMA Microparticles from Electrospaying.** The principle of electrospaying is well described in review papers.<sup>30-32</sup> Figure 1 shows the experimental setup for electrospaying in this study. A concentric co-axial nozzle (NanoNC, Korea) was used in this study. The PMMA nanoparticle dispersion in acetone (2 wt %) was supplied from a syringe pump (KD Scientific, Korea) into the inner nozzle. Compressed air was supplied in the outer nozzle (absolute pressure of 1.71 bar) to evaporate acetone rapidly. The sizes of the inner and the outer nozzles were 23G and 14G, respectively. 10 kV was applied for electrospaying from a power supply. The PMMA nanoparticles assembled into raspberry-like microparticles during electrospaying. The microparticles were collected on an aluminum foil.

The raspberry-like PMMA microparticles containing TiO<sub>2</sub> nanoparticles were prepared as follows. 2 g of PMMA nanoparticles and 0.4 g of TiO<sub>2</sub> powder were uniformly dispersed in 100 g of acetone. The dispersion was fed through the inner nozzle with a feeding speed of 10 mL/h at 10 kV while 1.71 bar of compressed air was steadily fed in the outer nozzle.

The raspberry-like PMMA microparticles containing methoxyphenyl triazine or ethyl(4-(2,3-dihydro-1*H*-indene-5-carboxyamido) benzoate) are known for UV-blocking and anti-aging functions in cosmetics, respectively.<sup>33</sup> To prepare using the same procedures described above, except that 0.4 g of either chemical was solubilized in 100 g of acetone containing 2 g of PMMA nanoparticles.

**Characterization.** Shapes of the PMMA nanoparticles

and the raspberry-like microparticles were observed by scanning electron microscopy (SEM). The UV-vis spectra of the powder microparticles containing TiO<sub>2</sub> or methoxyphenyl triazine were recorded using a UV-vis spectrophotometer (V-550, Jasco). An optical microscope (BX 50, Olympus) was used to observe the aqueous dispersion of microparticles containing ethyl(4-(2,3-dihydro-1*H*-indene-5-carboxyamido) benzoate). This experiment was conducted to investigate whether the bioactive drug was preserved stably in the microparticles without the formation of separate crystals in deionized water. The observation was performed after dispersion of the microparticles and storage in water for six weeks at 40 °C.

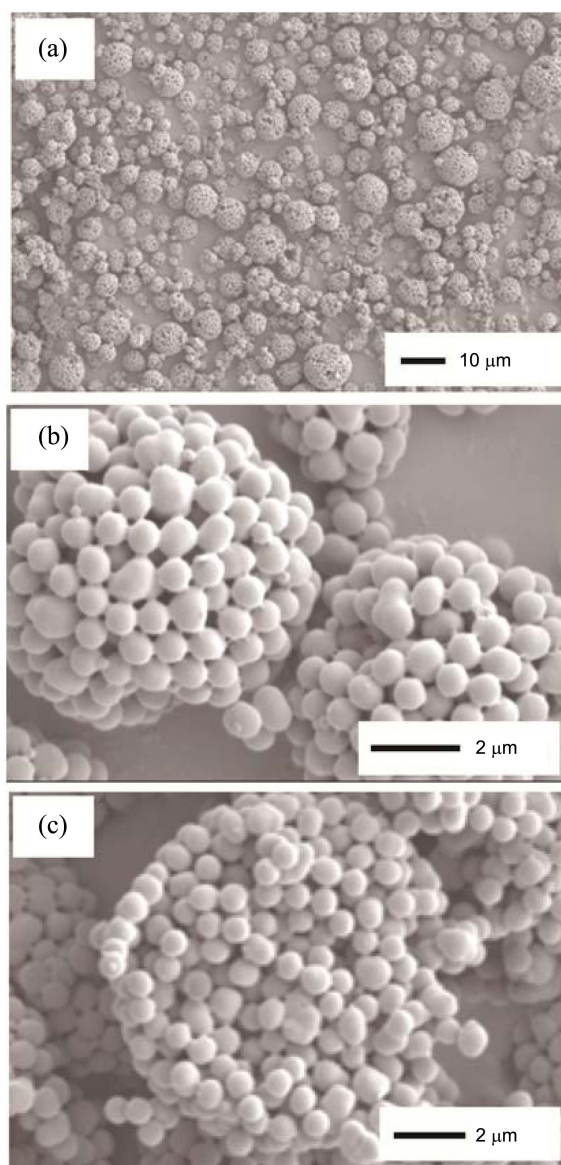


**Figure 2.** SEM images of the raspberry-like microparticles obtained by electrospaying the PMMA nanoparticles dispersed in acetone. A low magnification image showing the overall size distribution of the microparticles (a), a close-up image of the microparticles (b), and an image exhibiting the interior structure of the microparticles taken after being fractured by a razor blade.

## Results and Discussion

Figure 1 is a scheme illustrating the method used in this study. The raspberry-like structures were produced from the concentric co-axial electrospaying setup. The PMMA nanoparticles and functional materials dissolved in an organic solvent (either dispersed or solubilized) were sprayed from an inner nozzle under electric field while air flow was supplied from an outer nozzle. The PMMA nanoparticles in the solution were assembled during electrospaying to form spherical microspheres with raspberry-like structures and porous interiors. Electrospaying a mixture solution containing the PMMA nanoparticles and functional nanoparticles or organic molecules made possible encapsulation of various functional materials in the raspberry-like microparticles. The functional materials could be evenly distributed in the body of the raspberry-like microparticles or selectively accumulated on the surface of the microparticles. The overall distribution should depend on compatibility of the functional materials with the PMMA suspension when the PMMA nanoparticles were condensed due to solvent evaporation during electrospaying. If the material is crystallized at high concentration, the crystallization kinetics can govern the morphology because the crystallization can induce phase separation from the PMMA suspension.

Uniformly-sized PMMA nanoparticles (300 nm in diameter) were synthesized from dispersion polymerization in an M- $\beta$ -CD aqueous solution. The nanoparticles were cross-linked by the 10 mol % crosslinking agent (EGDMA) used for the synthesis. As a result, instead of being solubilized in acetone, PMMA nanoparticles were swollen and evenly dispersed. The raspberry-like microparticles were produced when the nanoparticle dispersion was fed into the inner nozzle under the electric field and the compressed air was supplied through the outer nozzle (see Figure 1). The nanoparticle dispersion formed a Taylor cone under the electric field and split into micron-sized droplets due to the Rayleigh instability.<sup>30-32</sup> Swollen PMMA nanoparticles within the drop assembled to form a raspberry-like structure during the rapid evaporation of acetone. Figure 2(a) shows a SEM image of the raspberry-like PMMA microparticles. From image analysis, the size of the microparticles was  $5.7 \pm 1.6$   $\mu\text{m}$ . The PMMA nanoparticles were packed to form a cluster, which is shown in Figure 2(b). Figure 2(c) shows the insides of the microparticles after being fractured with a razor blade. The nanoparticles assembled in a disordered manner, providing a porous interior. Since the crosslinked PMMA nanoparticles were swollen in acetone, they behaved like a gel containing acetone. During the assembly of the nanoparticles, it was thought that the polymer chains in the nanoparticles were physically entangled with the other polymer chains in the neighboring nanoparticles, leading to cohesion and hence to the formation of interconnected structure. The resulting raspberry-like particles were strong enough at high vortex flow.

Pore size of the microparticles could be reduced when smaller nanoparticles were incorporated in the microparticles.

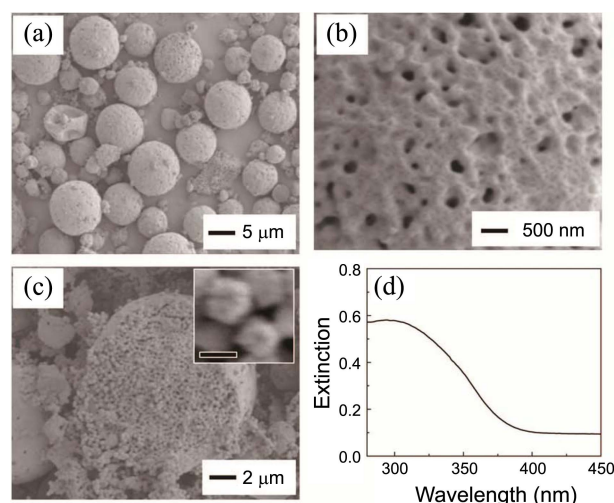


**Figure 3.** (a) A SEM image of the raspberry-like microparticles obtained by electrospaying an acetone suspension including the PMMA nanoparticles and titanium dioxide nanoparticles (30–50 nm). (b, c) SEM images showing (b) the surface and (c) interior microstructure of the a microparticle. Inset in (c) shows the close-up of the interior PMMA nanoparticles decorated with the TiO<sub>2</sub> nanoparticles (scale bar: 300 nm). (d) An UV-vis spectrum from dry powder of the microparticles. The spectrum displays the typical characteristics of the TiO<sub>2</sub> nanoparticles.

Figure 3(a) shows the microparticles prepared by electrospaying a dispersion of the PMMA nanoparticles and TiO<sub>2</sub> nanoparticles (30–50 nm; see Figure S1 in the Supporting Information for the TEM images of the TiO<sub>2</sub> nanoparticles). The size of the TiO<sub>2</sub>-containing microparticles was  $5.9 \pm 2.4$   $\mu\text{m}$  in diameter. The TiO<sub>2</sub>-containing microparticles had both micropores and mesopores ( $\sim 200$  nm) (Figure 3(b)). The interior of the microparticles (Figure 3(c)) were similar to that of the PMMA microparticles shown in Figure 2(d). However, a closer look at the individual microparticles (inset in Figure 3(c)) revealed that the surface of the PMMA nanoparticles were roughened, implying that the TiO<sub>2</sub> nanoparticles were embedded in the microparticles and adsorbed on the surface of the PMMA nanoparticles. Since PMMA is optically transparent, the raspberry-like microparticles are expected to retain the scattering function of the TiO<sub>2</sub> nanoparticles in the UV-B region (280–320 nm). This was confirmed by the UV-vis spectra from dried powder of microparticles containing the TiO<sub>2</sub> nanoparticles (Figure 3(d)).

Microparticles composed of the PMMA nanoparticles and methoxyphenyl triazine were also investigated. Methoxyphenyl triazine, tradename Tinosorb<sup>R</sup>-S, is used as an organic UV blocking compound. Methoxyphenyl triazine was solubilized in acetone, and the PMMA nanoparticles were dispersed in the solution. From the electrospaying, we obtained microparticles with sizes of  $3.2 \pm 1.0$   $\mu\text{m}$  (Figure 4(a)). The surfaces were nearly smooth with only a few nanosized pores (Figure 4(b)), but the interior structure of the microparticles was constructed by random arrangement of the PMMA nanoparticles (Figure 4(c)). The content of methoxyphenyl triazine was 17 wt % versus PMMA, which is supposed to be sufficient to protect the UV light in the region of

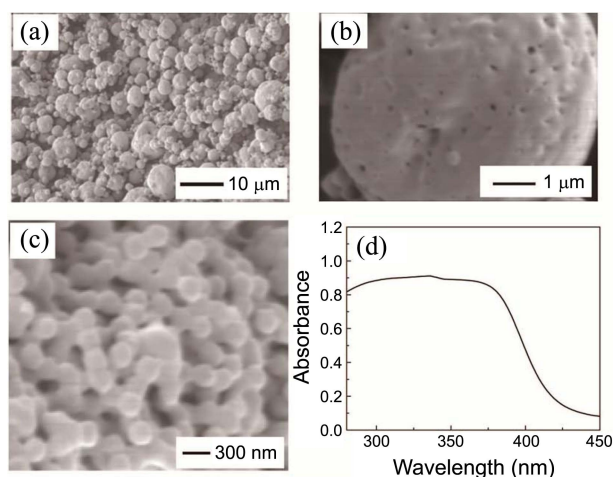


**Figure 4.** (a) A SEM image of the raspberry-like microparticles obtained by electro spraying an acetone suspension including the PMMA nanoparticles and methoxyphenyl triazine. (b, c) SEM images showing (b) the surface and (c) interior microstructure of a microparticle. (d) An UV-vis spectrum obtained from dry powder of the microparticles. The spectrum displays the typical characteristics of methoxyphenyl triazine.

280–400 nm (both UVA and UVB), as shown in Figure 4(d).

Figure 5 shows the microparticles containing ethyl(4-(2,3-dihydro-1*H*-indene-5-carboxyamido) benzoate). The sample preparation procedure was identical to that for the microparticles containing methoxyphenyl triazine. The overall structure of the microparticles (Figure 5(a)) was similar with those having no functional materials shown in Figure 2(c). Size of the microparticles was  $3.2 \pm 1.4$  μm. In addition, the crystal fibrils of ethyl(4-(2,3-dihydro-1*H*-indene-5-carboxyamido) benzoate) were observed on the surfaces of the microparticles (Figure 5(b)). Although the fibrils were also found in the interior of the microparticles, the population was much less than that on the surface (Figure 5(c)). The fibrils may result from the rapid crystallization of ethyl(4-(2,3-dihydro-1*H*-indene-5-carboxyamido) benzoate) followed by phase separation of the crystals from the PMMA nanoparticles during evaporation of the solvent. When compared with the morphology of the microparticles containing methoxyphenyl triazine, it was thought that the crystallization behavior and miscibility of the organic compounds with the PMMA nanoparticles greatly influence the surface and interior structures of the raspberry-like microparticles.

Although ethyl(4-(2,3-dihydro-1*H*-indene-5-carboxyamido) benzoate) retards the aging of skin,<sup>33</sup> the use of the compound has been limited because it is rapidly crystallized in aqueous systems and not compatible with typical encapsulating materials for cosmetics. Dissolution of the crystals and precipitation taking place later in the suspension hampers the stability of the emulsion and spoils the product. Therefore, widespread use of this compound depends on the stability of the compound in aqueous systems. An optical microscope was used to observe the aqueous dispersion of microparticles after the dispersion was stored for six weeks at 40 °C. As shown in Figure 5(d), ethyl(4-(2,3-dihydro-1*H*-indene-5-

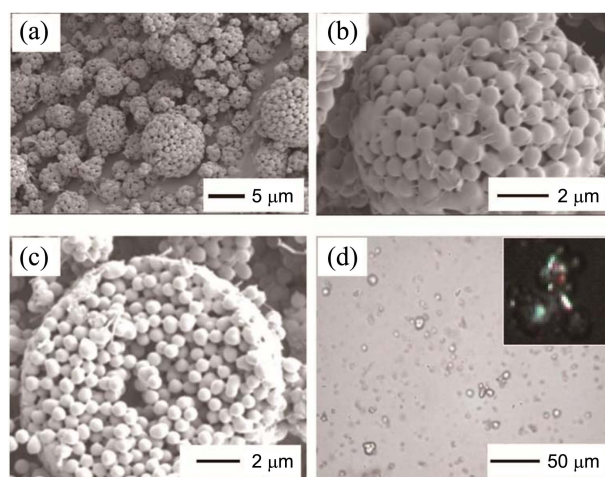


**Figure 5.** (a) A SEM image of the raspberry-like microparticles obtained by electro spraying an acetone suspension containing the PMMA nanoparticles and ethyl(4-(2,3-dihydro-1*H*-indene-5-carboxyamido) benzoate). (b, c) SEM images showing (b) the surface and (c) interior microstructure of a microparticle. (d) An optical microscope image showing the microparticles after storing the microparticles in deionized water for six weeks at 40 °C. The inset shows the dark field optical image exhibiting the crystals of ethyl(4-(2,3-dihydro-1*H*-indene-5-carboxyamido) benzoate) embedded on the surface of the microparticles.

carboxyamido) benzoate) kept entrapped in the microparticles. We could not detect any crystal extract in the water phase, which is crucial in cosmetic use.

## Conclusions

Raspberry-like microparticles embedding various functional materials were prepared by electro spraying a suspension containing polymer nanoparticles and the target functional materials. The suspension was introduced through the inner nozzle of a concentric co-axial nozzle. Supplying compressed air in the outer nozzle helped production of copious amount of the microparticles with fast solvent evaporation. The microparticles produced from the random assembly of the nanoparticles were porous both on the surface and in the interior of the microparticles. This porous nature enabled a high payload of various functional materials (17 wt %). In this study, we embedded TiO<sub>2</sub> nanoparticles, methoxyphenyl triazine, and ethyl(4-(2,3-dihydro-1*H*-indene-5-carboxyamido) benzoate). Depending on the miscibility of the functional materials to the suspension of PMMA nanoparticles, the resulting surface and interior structures of the functional microparticles were different, leading to random distribution in whole body of the microparticles or preferential deposition on the surfaces of the microparticles. The results clearly suggest that the process to prepare the raspberry-like microparticles can be one of excellent approach to generate functional microstructures. We expect the process can be used to produce the same raspberry-like structures with stimuli-responsive particles such as PNIPAm hydrogel particles. A previous report suggested that water insoluble hydrophobic drugs could be loaded with high payload in porous structures

made of hydrogel particles.<sup>34</sup> Raspberry-like PNIPAm micro-particles will be further studied in the future work to prepare a stimuli-responsive delivery system.

**Acknowledgments.** This work was supported by a grant from Hanyang University (Grant 201300000001459). The authors acknowledge Amorepacific Corporation for technical support.

**Supplementary Materials.** A figure showing the transmission electron microscopy image of the TiO<sub>2</sub> nanoparticles is included in the supplementary material.

### References

- Whitesides, G. M.; Grzybowski, B. A. *Science* **2002**, *295*, 2418-2421.
- Stewart, M. E.; Anderton, C. R.; Thompson, L. B.; Maria, J.; Gray, S. K.; Rogers, J. A.; Nuzzo, R. G. *Chem. Rev.* **2008**, *108*, 494-521.
- Cho, E. C.; Kim, J.-W.; Fernández-Nieves, A.; Weitz, D. A. *Nano Lett.* **2008**, *8*, 168-172.
- Joannopoulos, J. D.; Villeneuve, P. R.; Fan, S. *Nature* **1997**, *386*, 143-149.
- Colvin, V. L. *MRS Bulletin* **2001**, 637-641.
- Debord, J. D.; Lyon, L. A. *J. Phys. Chem. B* **2000**, *104*, 6327-6331.
- Barthlott, W.; Neinhuis, C. *Planta* **1997**, *202*, 1-8.
- Ganesh, V. A.; Raut, H. K.; Nair, A. S.; Ramakrishna, S. *J. Mater. Chem* **2011**, *21*, 16304-16322.
- Guo, S.; Dong, S.; Wang, E. *J. Phys. Chem. C* **2009**, *113*, 5485-5492.
- Kind, L.; Plamper, F. A.; Gobel, R.; Manton, A.; Muller, Pieles, A. H. E. U.; Andreas, T.; Meier, W. *Langmuir* **2009**, *25*, 7109-7115.
- Chen, M.; Wu, L.; Zhou, S.; You, B. *Macromolecules* **2004**, *37*, 9613-9619.
- Chen, M.; Zhou, S.; You, B.; Wu, L. A. *Macromolecules* **2005**, *38*, 6411-6417.
- Wang, J.; Yang, X. *Langmuir* **2008**, *24*, 3358-3364.
- Perro, A.; Reculosa, S.; Bourgeat-Lami, E.; Duguet, E.; Ravaine, S. *Colloids and Surf. A* **2006**, *78*, 284-285.
- Qiao, X.; Chen, M.; Zhou, J.; Wu, L. *J. Polym. Sci. Part A* **2007**, *45*, 1028-1037.
- Shi, S.; Zhou, L.; Wang, T.; Bian, L.; Tang, Y.; Kuroda, S.-I. *J. Appl. Polym. Sci.* **2011**, *120*, 501-508.
- Choi, W. S.; Koob, H. Y.; Huck, W. T. S. *J. Mater. Chem.* **2007**, *17*, 4943-4946.
- Yu, M.; Wang, H.; Zhou, X.; Yuan, P.; Yu, C. *J. Am. Chem. Soc.* **2007**, *129*, 14576-14577.
- Wu, X.; Tian, Y.; Cui, Y.; Wei, L.; Wang, Q.; Chen, Y. *J. Phys. Chem. C* **2007**, *111*, 9704-9708.
- Wang, C.; Yan, J.; Cui, X.; Wang H. *J. Colloid Interf. Sci.* **2011**, *354*, 94-99.
- Schrade, A.; Cao, Z.; Landfester, K.; Ziener, U. *Langmuir* **2011**, *27*, 6689-6700.
- Ming, W.; Wu, D.; Benthem, R. V.; With, G. D. *Nano Lett.* **2005**, *5*, 2298-2301.
- Qian, Z.; Zhang, Z.; Song L.; Liu, H. *J. Mater. Chem.* **2009**, *19*, 1297-1304.
- D'Acunzi, M.; Mammen, L.; Singh, M.; Deng, X.; Roth, M.; Auernhammer, G. K.; Butt, H.-J.; Vollmer, D. *Faraday Discuss.* **2010**, *146*, 35-48.
- Puretskiy, N.; Ionov, L. *Langmuir* **2011**, *27*, 3006-3011.
- Tsai, H.-J.; Lee, Y.-L. *Langmuir* **2007**, *23*, 12687-12692.
- Li, Z.; Ravaine, V.; Ravaine, S.; Garrigue, P.; Kuhn, *Adv. Funct. Mater.* **2007**, *17*, 618-622.
- Pastoriza-Santos, I.; Gomez, D.; Pérez-Juste, J.; Liz-Marzán, L. M.; Mulvaney, P. *Phys. Chem. Chem. Phys.* **2004**, *6*, 5056-5060.
- Storsberg, J.; Aert, H. V.; Roost, C. V.; Ritter, H. *Macromolecules* **2003**, *36*, 50-53.
- Li, D.; Xia, Y. *Adv. Mater.* **2004**, *16*, 1151-1170.
- Greiner, A.; Wendorff, J. H. *Angew. Chem. Int. Ed.* **2007**, *46*, 5670-5703.
- Sill, T. J.; Recum, H. A. V. *Biomaterials* **2008**, *29*, 1989-2006.
- Yoo, J. W.; Rho, H. S.; Kim, S. J.; Yoon, J. W.; Ahn, S. Y.; Kim, D. H. *KRI00786300*, 2007.
- Cho, E. C.; Hyun, D. C.; Jeong, U.; Kim, J.-W.; Weitz, D. A. *Langmuir* **2010**, *26*, 3854-3859.